

## Microstructures and mechanical properties of tungsten wire/particle reinforced $Zr_{57}Nb_5Al_{10}Cu_{15.4}Ni_{12.6}$ metallic glass matrix composites

Haein Choi-Yim,<sup>a)</sup> Jan Schroers, and William L. Johnson  
W.M. Keck Laboratory of Engineering Materials, Mail Code 138-78, California Institute of Technology,  
Pasadena, California 91125

(Received 27 September 2001; accepted for publication 24 January 2002)

Tungsten wire or particle reinforced metallic glass matrix composites are produced by infiltrating liquid  $Zr_{57}Nb_5Al_{10}Cu_{15.4}Ni_{12.6}$  (Vit106) into tungsten reinforcements at 1150 and at 1425 K. X-ray diffraction, differential scanning calorimetry, and scanning electron microscopy are carried out to characterize the composite. The matrix of the composite processed at 1150 K is mostly amorphous, with some embedded crystals. During processing, tungsten dissolves in the glass-forming melt and upon quenching precipitates over a relatively narrow zone near the interface between the tungsten and matrix. In the composites processed at 1425 K, tungsten dissolves in the melt and diffuses through the liquid medium, and then reprecipitates upon quenching. The faster kinetics at this high temperature results in a uniform distribution of the crystals throughout the matrix. Mechanical properties of the differently processed composites containing wires and particles are compared and discussed. The composites exhibit a plastic strain failure of up to 16% without sacrificing the high-failure strength, which is comparable to monolithic Vit106. © 2002 American Institute of Physics. [DOI: 10.1063/1.1459766]

The limited plasticity of monolithic bulk metallic glasses (BMGs) has triggered research on metallic glass matrix composites. To improve the toughness two different approaches have been followed. One is to introduce foreign particles into the matrix. It was found that a variety of reinforcement materials such as SiC, WC, Ta, or W can be introduced into the metallic glass matrix without inducing crystallization.<sup>1-6</sup> The size of these particles ranges from 3 to 100  $\mu\text{m}$ . One crucial contribution to improve the ductility is the formation of a strong interface between the reinforcement material and BMG.<sup>7</sup> To guarantee a strong interface another approach has been followed where the composite forms *in situ*. This is done by partially crystallizing the sample upon cooling<sup>8</sup> or upon subsequent heating.<sup>9</sup> The size of these reinforcement crystals varies between several nm to 20  $\mu\text{m}$ . Volume fraction of the reinforcement crystals can be controlled by varying composition, processing time, and temperature, though not as directly as in the case of direct addition of particles to the glass-forming melt.

The  $Zr_{57}Nb_5Al_{10}Cu_{15.4}Ni_{12.6}$  (Vit106) glass-forming alloy is one of the best glass-forming Zr-based alloys that does not contain Be.<sup>10</sup> In addition, it is very robust against heterogeneous nucleation at surfaces or interfaces. The thermal stability of this alloy with respect to crystallization is not compromised by adding crystalline particles into its molten state.<sup>11</sup> The plastic deformation range under compression of the glass was improved by 300% when WC, W, or Ta particles with only 5%–10% volume fraction were added to it.<sup>12</sup> This is attributed to the fact that the material no longer fails along a single shear band that traverses the sample but forms multiple shear bands in the presence of particles.

In this letter, we combine the techniques of adding foreign particles and *in situ* composite formation. Thermal and microstructure investigations are presented for tungsten me-

tallic glass composites processed at 1150 and 1425 K. The high-processing temperature of 1425 K was chosen in order to increase the amount of tungsten that dissolves in the melt during processing the Vit106 liquid. Upon cooling, tungsten precipitates out and forms uniformly distributed crystals that result in a dense array of tungsten crystals in the Vit106 matrix. We will show that the composite sample processed at 1425 K contained more than 15 at. % of tungsten dissolved in the matrix prior to cooling. The effect of increasing tungsten dissolution into the matrix on the mechanical properties of these composites is presented and discussed.

Ingots of  $Zr_{57}Nb_5Al_{10}Cu_{15.4}Ni_{12.6}$  were made by arc melting a mixture of the elemental metals (purity better than 99.5%, metal basis). Tungsten wires, with a nominal diameter of 250  $\mu\text{m}$ , were straightened and cut to 5 cm lengths. In addition, tungsten powders with an average diameter of 80  $\mu\text{m}$  were used as reinforcement. Composite specimens were cast in a resistive furnace by melting the ingots in an evacuated 7-mm-inner-diam 304 stainless-steel tube packed with wire or particle reinforcement, followed by pressure infiltration of the molten Vit106 alloy. The reinforcement particles were placed in the sealed end of the tube, which was necked about 2 cm above the reinforcement. Ingots of the matrix materials were placed in the tube above the neck. Prior to heating, the tube was evacuated and then flushed with argon gas several times to remove residual oxygen. The sample tube was heated under vacuum in a resistive tube furnace with temperature feedback control to minimize trapped gas in the composite sample. The sample was then heated to 1250 K, well above the liquids temperature of 1093 K of the Vit106 alloy. This overheating of the molten Vit106 is found useful in dissolving residual oxides and other impurities that degrade the glass-forming ability of the alloy.<sup>13</sup> The sample was held at this temperature for 10 min. The temperature was then lowered to 1150 K and allowed to stabilize. When the furnace reached this target temperature, a pressure of 80 psi

<sup>a)</sup>Electronic mail: hchoi@its.caltech.edu

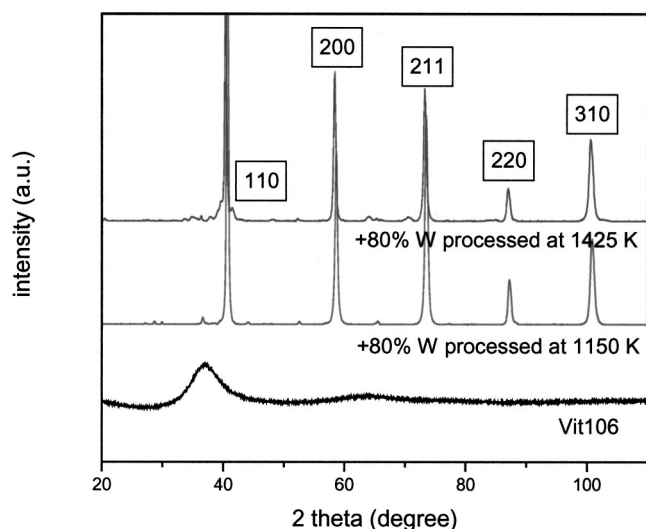


FIG. 1. X-ray diffraction patterns of monolithic Vit106 and tungsten wire reinforced Vit106 composites processed at 1150 and 1425 K.

argon was applied above the melt. These conditions were held for 15 min to allow infiltration of the molten matrix material into the reinforcement. Subsequently, the sample was quenched in water. The samples processed at 1425 K were heated directly to this temperature, held for 15 min, and then subjected to infiltration under pressure.

Each composite sample was examined by differential scanning calorimetry (DSC) and its cross section by x-ray diffraction. The microstructure of the composite was studied by scanning electron microscopy (SEM) and electron microprobe.

Quasistatic compression tests were performed on a universal testing machine (Instron 4200) with constant strain rates between  $8 \times 10^{-5}$  and  $3 \times 10^{-4} \text{ s}^{-1}$ . The strains were measured with strain gauges placed directly on the surface of the cylindrical samples, which had a diameter of 3 mm and an aspect ratio of 2–2.2. The ends of the cylinders were ground flat and perpendicular to the loading axis. Two samples of each material were tested under identical conditions.

Figure 1 shows the x-ray diffraction patterns of monolithic Vit106 and tungsten wire reinforced composites processed at 1150 and at 1425 K. The pattern of the monolithic Vit106 exhibits the broad peak characteristic for the amorphous structure. The diffraction pattern of the composite processed at 1150 K shows, in addition to the intense peaks of the reinforcement material, several small peaks that do not belong to the x-ray spectra of the reinforcement material. The broad diffraction maxima of the amorphous phase is somewhat obscured by the narrow peaks of the crystalline phases with their higher intensities. The diffraction pattern of the composite processed at 1425 K shows more small crystalline peaks, which do not belong to the diffraction pattern of the reinforcement particles, indicating the formation of more crystalline phases. Peak positions of the additional crystalline phases differ for wire and particle reinforcement composite, indicating crystallization of different phases.

DSC investigations were carried out to determine the amount of material that crystallized upon cooling. The results are summarized in Table I. By comparing the heat released

TABLE I. Crystallization temperature, heat releases, and amorphous volume fraction after processing for monolithic Vit106 and tungsten reinforced Vit106 composites processed at 1150 and 1425 K.

Material	$T_x$ (K)	$\Delta H$ (J/g)	Volume fraction amorphous (%)
Vit106, monolithic	760	24.7	100
Vit106+50% W particles, 1150 K	753	4.1	35
Vit106+80% W wire, 1150 K	753	2.9	18
Vit106+50% W particles, 1425 K	748	3	25
Vit106+80% W wire, 1425 K	...	...	0

upon heating of the monolithic Vit106 of 24.7 J/g, we can conclude that for the Vit106+50% particles processed at 1150 K about 65% of the Vit106 liquid has crystallized. In the Vit106+80% wire composite 18% of the Vit106 liquid remains amorphous. Processing at 1425 K leads to complete crystallization of the 80% wire composite but the 50 vol % particle composite still contains a 25% amorphous volume fraction.

Figure 2(a) shows the SEM image of the interfacial region between a tungsten wire and the amorphous Vit106 matrix processed at 1150 K. The matrix appears uniform and free of heterogeneity. According to wavelength-dispersive x-ray (WDX) analysis, 0.4 at. % of tungsten is dissolved on average in the matrix. The composition of the matrix is very close to the Vit106 composition. In a several-micron-thick layer near the glass/tungsten-wire interface, about 10 at. % tungsten was measured.<sup>13</sup> The composite processed at 1425 K is shown in Fig. 2(b). In the area between the reinforcement wires a large number of small crystalline particles are distributed in the matrix. The microstructure suggests that upon cooling the solubility of tungsten in Vit106 is exceeded, where it precipitates uniformly over the matrix.

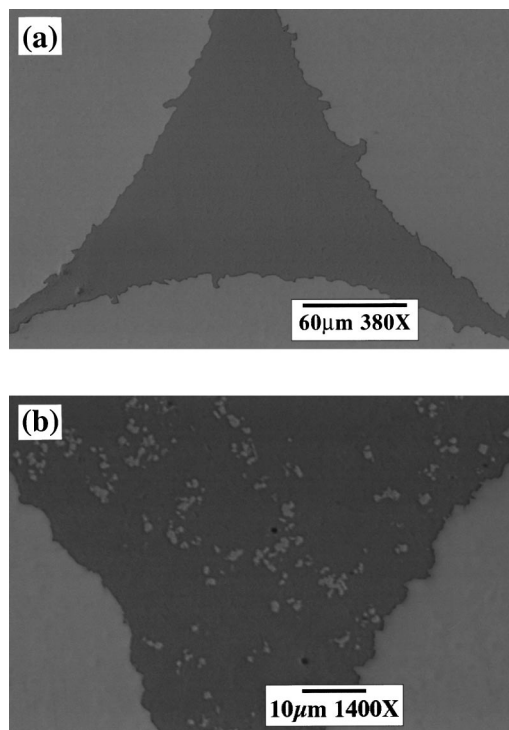


FIG. 2. SEM backscattering image of Vit106+W wire composite processed at (a) 1150 K and (b) 1425 K.

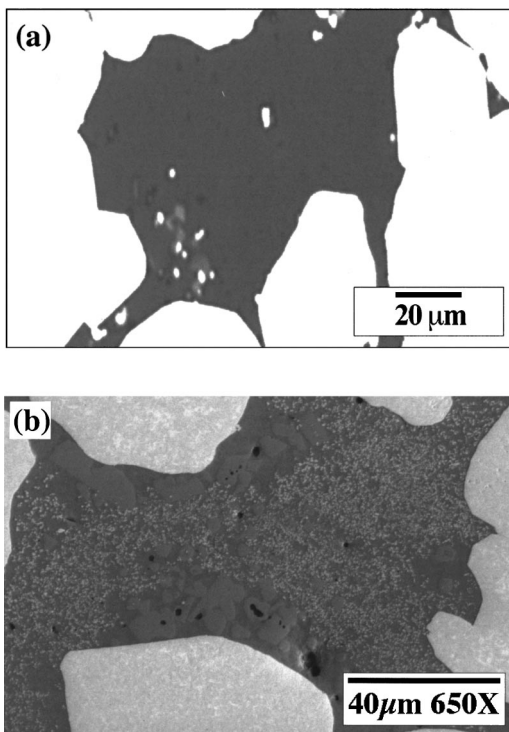


FIG. 3. SEM backscattering image of the Vit106+W particle composite processed at (a) 1150 K and (b) 1425 K.

Similar tungsten dissolution was found in the composite with tungsten particles. Figure 3(a) depicts the SEM image of the area between the tungsten particles and the Vit106 matrix processed at 1150 K. Tungsten particles of various sizes around  $80\ \mu\text{m}$  were used to reinforce the Vit106. The composition of the matrix is very close to the Vit106 composition and 0.2 at. % of tungsten is dissolved in the matrix. In the composite processed at 1425 K, as shown in Fig. 3(b), a large number of particles with the size of  $1\ \mu\text{m}$  formed uniformly in the matrix. WDX analysis is not capable of accurately measuring the composition of  $1\text{-}\mu\text{m}$ -size particles. However, in order to estimate their composition, we performed measurements on several different particles. From this we can conclude that  $1\ \mu\text{m}$  particles consist of substantially more W and less Zr compared to nominal composition of Vit106. Larger crystals of about  $10\ \mu\text{m}$  in diameter with compositions of 64.4 at. % Zr, 5.6 at. % Nb, 5 at. % Al, 11.5 at. % Ni, 8.5 at. % Cu, and 4.9 at. % W form preferentially in the neighborhood of the reinforcement material. The compositions of the matrix of 57.4 at. % Zr, 2.8 at. % Nb, 8.6 at. % Al, 14 at. % Ni, 16.8 at. % Cu, and 0.2 at. % W, are very close to the Vit106 composition.

Compression tests were performed on monolithic Vit106 and composites containing tungsten wires and tungsten particles processed at 1150 and 1425 K. They are depicted in Fig. 4. Unreinforced Vit106 exhibits only 0.5% plastic deformation in compression. The tungsten wire reinforced composites processed at 1150 K showed extremely large compressive strains to failure of up to 16.2%. The total strain to failure is a factor of 6 larger than for the case of unreinforced Vit106. In contrast, the composite with tungsten wire processed at 1425 K shows only 3% plasticity and less ultimate strength and strain to failure. This might be caused by the complete crystallization of the matrix to a brittle phase. The

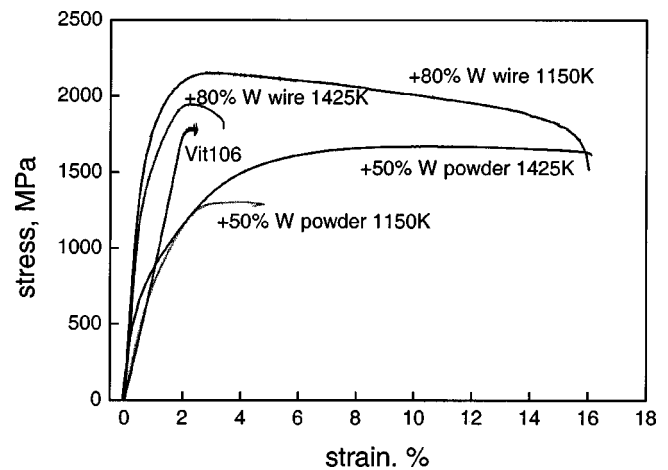


FIG. 4. Compressive strain and stress curves of monolithic Vit106 and Vit106+W wire and Vit106+W particles composite processed at 1150 and 1425 K.

composite with tungsten particles processed at 1425 K shows dramatically increased plasticity compared to the composite with tungsten particles processed at 1150 K. The ultimate strength of the composite materials is increased significantly and the strains to failure are increased to a value of about 16%. An explanation for this improvement may be the higher density of tungsten crystals in the Vit106 matrix. The bimodal crystal size distribution might also affect shear band formation and propagation, and therefore, the plasticity.

In summary, composites of  $\text{Zr}_{57}\text{Nb}_5\text{Al}_{10}\text{Cu}_{15.4}\text{Ni}_{12.6}$  with tungsten were processed at 1150 and 1425 K. During processing tungsten dissolves into the liquid. The amount of tungsten dissolved increases with increasing process temperature and is higher for wire reinforcement material than for particle reinforcement material. Upon cooling the tungsten particles precipitate in the form of the bcc phase. If the tungsten fraction in the liquid is too high, the entire liquid crystallizes. The composites with tungsten particles processed at 1425 K and the tungsten wire reinforced Vit106 processed at 1150 K, exhibit a dramatic increase in plasticity, resulting in a ductile material.

The authors would like to thank Dr. Szuets for his contributions to this investigation. This work was supported by the U.S. Army Research Office under Grant No. DAAD19-01-1-0525.

- <sup>1</sup>H. Choi-Yim and W. L. Johnson, *Appl. Phys. Lett.* **71**, 3808 (1997).
- <sup>2</sup>H. Kato and A. Inoue, *Mater. Trans., JIM* **38**, 793 (1997).
- <sup>3</sup>R. D. Conner, R. B. Dandliker, and W. L. Johnson, *Acta Mater.* **46**, 6089 (1998).
- <sup>4</sup>J. Eckert, A. Kubler, and L. Schultz, *J. Appl. Phys.* **85**, 7112 (1999).
- <sup>5</sup>C. Fan, D. V. Louzguine, C. F. Li, and A. Inoue, *Appl. Phys. Lett.* **75**, 340 (1999).
- <sup>6</sup>Y. Kawamura, H. Mano, and A. Inoue, *Scr. Mater.* **43**, 1119 (2000).
- <sup>7</sup>J. Schroers, K. Samwer, F. Szuets, and W. L. Johnson, *J. Mater. Res.* **15**, 1617 (2000).
- <sup>8</sup>C. C. Hays, C. P. Kim, and W. L. Johnson, *Phys. Rev. Lett.* **84**, 2901 (2000).
- <sup>9</sup>A. Inoue, T. Zhang, and Y. H. Kim, *Mater. Trans., JIM* **38**, 749 (1997).
- <sup>10</sup>X. H. Lin, Ph.D. thesis, California Institute of Technology (1997).
- <sup>11</sup>H. Choi-Yim, R. Busch, and W. L. Johnson, *J. Appl. Phys.* **83**, 7993 (1998).
- <sup>12</sup>H. Choi-Yim, R. Busch, and W. L. Johnson, *Acta Mater.* **47**, 2455 (1999).
- <sup>13</sup>R. B. Dandliker, Ph.D. thesis, California Institute of Technology (1998).